Scripta Materialia 131 (2017) 6–10

Contents lists available at ScienceDirect

Scripta Materialia

journal homepage: www.elsevier.com/locate/scriptamat

Regular article

Capacity and mechanisms of plastic deformation in β-$Lu_2Si_2O_7$

Zhilin Tian [a,b], Liya Zheng [a], Jiemin Wang [a], Jingyang Wang [a,*]

[a] Shenyang National Laboratory for Materials Science, Institute of Metal Research, Chinese Academy of Sciences, Shenyang 110016, China
[b] University of Chinese Academy of Sciences, Beijing 100049, China

ARTICLE INFO

Article history:
Received 17 October 2016
Received in revised form 14 December 2016
Accepted 15 December 2016
Available online xxxx

Keywords:
Rare earth silicates
Fiber-matrix interphase
Deformation mechanism

ABSTRACT

$RE_2Si_2O_7$ disilicates are promising candidates for oxidation resistant interfacial phase in SiC fiber-reinforced SiC matrix composites due to their good damage tolerance, good phase stability and compatible thermal expansion coefficients with SiC. We herein investigate the capacity and mechanisms of plastic deformation in β-$Lu_2Si_2O_7$ by a combination of Hertzian indentation experiment and transmission electron microscopy observation. A large amount of (1 1 0) deformation twinning, dislocations and slip bands are observed. For the common twinning mode, fewer atomic shuffle types, small shear strain, and low shear modulus in the twinning direction help explain the prevalence of this mode.

Lightweight high-performance SiC fiber-reinforced SiC matrix composites (SiC_f/SiC) are promising material for use as high-pressure turbine shrouds and combustor liners in engines, structural components in aerospace applications, and fuel cladding in fusion reactors due to their pseudo-ductile fracture and high reliability [1,2]. During failure in SiC_f/SiC, complicated fracture modes including fiber pullout, fiber fracture and interfacial debonding will take place. SiC fibers were usually coated with carbon and BN to obtain the optimized SiC_f/SiC. However, the application of SiC_f/SiC is often limited by mechanical property degradation due to the oxidation of BN or carbon fiber-matrix interphases in oxidizing environment [3,4]. Approaches would be to replace BN or carbon with a functionally equivalent but oxidation-resistant material. Hay et al. have explored some oxide ceramics as weakly bonded fiber-matrix interphases, such as ZrO_2-SiO_2 [5], $REPO_4$ (RE = rare earth) [6,7], and γ-$Y_2Si_2O_7$ [8]. $LaPO_4$ and γ-$Y_2Si_2O_7$ show extensive plastic deformations under external loads [3], but the $LaPO_4$ coating on SiC fibers decomposes in reducing atmospheres at high temperatures during processing SiC_f/SiC [9] and γ-$Y_2Si_2O_7$ undergoes phase transition at high temperatures which limited their practical applications [10]. Recently, β-$Lu_2Si_2O_7$ was found a damage tolerant ceramic with high melting point (1900 °C) [11], no phase transition, and low thermal expansion coefficients [12], which suggests it may be a promising oxidation-resistant fiber-matrix interphase in SiC_f/SiC. It is well established that the mechanical behavior of SiC_f/SiC mainly depends on the properties of fiber-matrix interface. To obtain enhanced toughness through fiber reinforcement, the fiber-matrix interphase must exhibit excellent capability of plastic deformation [3]. Deformation mechanisms including dislocations and twinning in monazite have been comprehensively investigated [7]. In γ-$Y_2Si_2O_7$, only slip bands, stacking faults and dislocations were found in deformed samples, however, no twinning modes were observed, by far [13,14]. In addition, very little deformation twinning or dislocation slip in α-$Y_2Si_2O_7$ and β-$Y_2Si_2O_7$ were discovered [3]. Similar with γ-$Y_2Si_2O_7$, β-$Lu_2Si_2O_7$ is constructed by corner sharing [SiO_4] tetrahedra and [REO_6] polyhedra as well, therefore, influences on properties can be explained by considering the configuration of these two units. Nevertheless, the deformation mechanisms in β-$Lu_2Si_2O_7$ are unclear.

In this work, Hertzian indentation test was conducted at room temperature to introduce deformation into bulk β-$Lu_2Si_2O_7$ sample. Transmission electron microscopy (TEM) observation was further used to characterize the deformation mechanisms of the indented β-$Lu_2Si_2O_7$ sample. In addition, density functional theory (DFT) calculation was carried out to calculate the second order elastic constants which were used for the shear modulus analysis. In the low stress deformed zone, a large amount of twinning, dislocations and slip bands were found. Twinning modes were predicted and compared with the result from experimental observation. The obtained results provide a deeper understanding of the deformation mechanisms in rare earth disilicates.

Pure phase and dense β-$Lu_2Si_2O_7$ bulk samples were prepared by hot pressing method [12]. Bulk β-$Lu_2Si_2O_7$ samples with dimension of about 3 mm × 4 mm × 4 mm were indented by a spherical Si_3N_4 indenter with a diameter of 8 mm. The indenter was attached to a universal testing machine with a crosshead speed of 0.05 mm·min^{-1}. Nanoindentation test was carried with Agilent Nano Indenter G200. Samples for TEM analysis were prepared from regions containing indentations by polishing the face opposite to the indented surface, mounting the polished slices on copper grids, and ion-milling at 4 kV. A 200 kV Tecnai

* Corresponding author.
E-mail address: jywang@imr.ac.cn (J. Wang).

http://dx.doi.org/10.1016/j.scriptamat.2016.12.023
1359-6462/

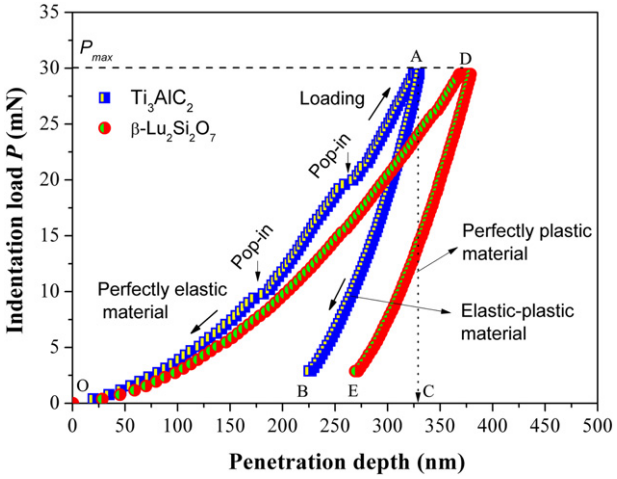

Fig. 1. Nanoindentation load-displacement curves of β-$Lu_2Si_2O_7$ and Ti_3AlC_2.

G^2 F20 TEM (FEI, Eindhoven, the Netherlands) was used for both selected area electron diffraction (SAED) and high-resolution TEM (HRTEM) analysis.

It is well known that Ti_3AlC_2 is a representative MAX phase with good damage tolerance and plasticity. To compare the mechanical response between β-$Lu_2Si_2O_7$ and Ti_3AlC_2, the load-displacement curves of them were obtained by nanoindentation test as shown in Fig. 1. The load-displacement curve can reflect whether a body behaves elastically (brittle), elastic-plastically, or plastically (ductile). The loading and unloading segments in the curve of Ti_3AlC_2 were marked as OA and AB respectively. Thus, the area A_1 (OAB) represents the plastic work while the area A_2 (BAC) is elastic recovery of a viscoelastic-plastic material. In case of purely plastic material, area $A_2 = 0$, and the unloading curve is a straight line. For perfectly elastic material the unloading curve follows the same curve as loading curve resulting in 100% recovery [15]. MAX phases possess high toughness and good damage tolerance which are recognized to bridge the property gap between metals and ceramics [16]. One can find that the area representing the plastic work of β-$Lu_2Si_2O_7$ is close to that of Ti_3AlC_2, which fully illustrates the quasi-plastic characteristic of β-$Lu_2Si_2O_7$. In addition, some pronounced displacement pop-ins (strain avalanche) can be detected in the loading curve of Ti_3AlC_2, but not in that of β-$Lu_2Si_2O_7$. The sudden displacement excursion is a result of plasticity onset, immediately after perfect elasticity process [17]. Therefore, it suggests that β-$Lu_2Si_2O_7$ show less plasticity than MAX phases. Similar with MAX phases, β-$Lu_2Si_2O_7$ can be described as sandwich-like layered stack of [Si_2O_7] units and [LuO_6] units. The layered structure results in the quasi-plastic of β-$Lu_2Si_2O_7$.

Hertzian indentation test was used to study the capability of plastic deformation. The sample was indented at a load of 1 kN with a spherical indenter. The microstructures of deformation regions under the Hertzian indentation zone were investigated by TEM. Fig. 2 displays the TEM images of low stress deformed zone. A large amount of deformation twinning, dislocations and slip bands were frequently observed. Fig. 2(a), (b) and (c) show the TEM bright field image of deformation twinning and its corresponding SAED patterns in β-$Lu_2Si_2O_7$, and Fig. 2(d) shows the slip bands. Boakye illustrated that plastic deformation in β-$Y_2Si_2O_7$ was less apparent. Due to smaller grain size in β-$Y_2Si_2O_7$, Nabarro-Herring or Coble creep mechanisms were more common, with less extensive evidence of dislocation slip or deformation twinning [3]. β-$Lu_2Si_2O_7$ has the same crystal structure as β-$Y_2Si_2O_7$. But the average grain size of β-$Lu_2Si_2O_7$ is 10 μm which is about 50 times larger than that of β-$Y_2Si_2O_7$ (0.2 μm) [18]. Large grain size promotes slip and twinning within grains [19]. In β-$Lu_2Si_2O_7$, twinning is more common than slip band. Most twinning is on (1 1 0). Twinning is an important deformation mechanism in low symmetry ceramic that possesses few slip

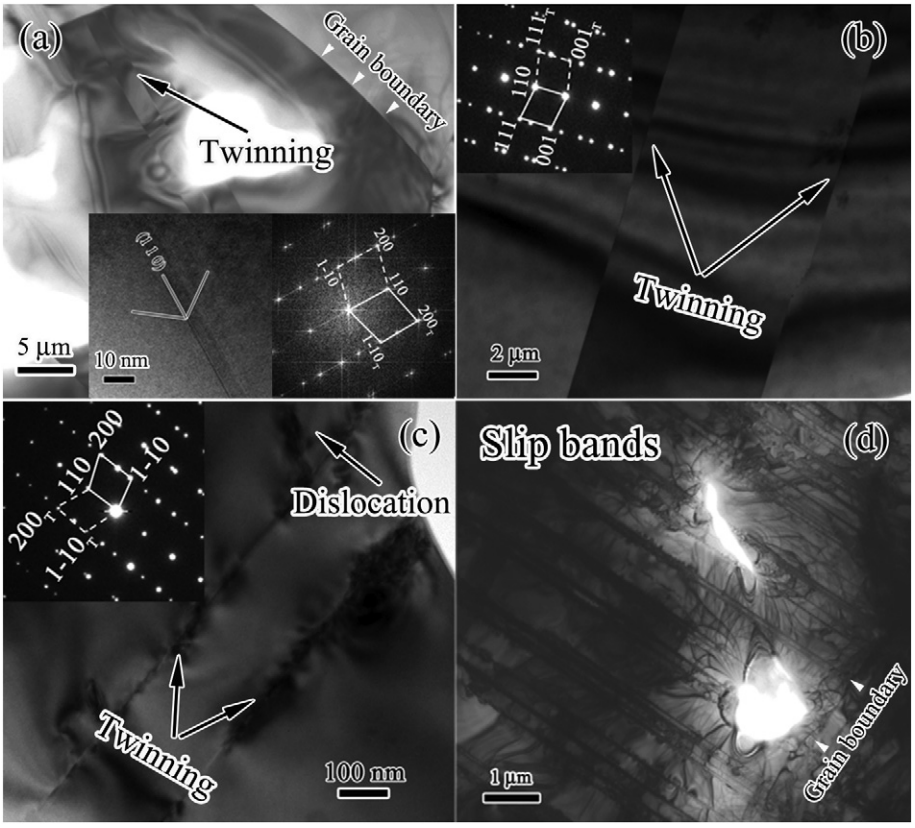

Fig. 2. TEM images of deformation twinning in (a) to (c) and slip bands in (d).